Accelerated singlet energy transfer in bis(phenylethynyl)phenylene-bridged 5,10,15,20-tetraaryl zinc–free base hybrid diporphyrins

PERKIN 2

Atsuhiro Osuka,*[a] Masako Ikeda,[a] Hideo Shiratori,[a] Yoshinobu Nishimura[b] and Iwao Yamazaki[b]

[a] *Department of Chemistry, Graduate School of Science, Kyoto University, Kyoto 606-8502, and Core Research for Evolutional Science and Technology (CREST) of Japan Science and Technology Corporation (JST), Japan*
[b] *Department of Chemical Process Engineering, Graduate School of Engineering, Hokkaido University, Sapporo 060-8628*

Received (in Cambridge) 29th October 1998, Accepted 5th March 1999

A set of three bis(phenylethynyl)phenylene-bridged 5,10,15,20-tetraaryl zinc–free base hybrid diporphyrins **1–3(ZH)** has been prepared by the Pd-catalyzed coupling reaction of ethynyl-substituted zinc–porphyrin **7** with diiodobenzene derivatives followed by partial zinc-insertion and separation by chromatography over a silica gel flash column. A similar reaction of **7** with 1,2,4,5-tetraiodobenzene effectively provided porphyrin tetramer **10** in 16% yield in a single step. Intramolecular singlet energy transfer in zinc–free base hybrid diporphyrins **1–3(ZH)** has been studied by picosecond time-resolved fluorescence spectroscopy. Determined intramolecular energy transfer rates (k_{EN}) are 1.5×10^{10} s^{-1}, 4.6×10^{9} s^{-1}, and 6.4×10^{9} s^{-1}, respectively, being larger than those of the corresponding 10,20-diaryl-2,3,7,8,12,13,17,18-octaalkyl-substituted diporphyrins. The k_{EN} rate enhancement has been found to depend on the geometry of the two porphyrins; 3.4-, 8.1-, and 11-fold for 1,2-, 1,3-, and 1,4- isomers, respectively, reflecting the magnitude of the through-bond electronic interactions.

In recent years, considerable attention has been focused on energy- and electron-transfer reactions in donor–acceptor systems bridged by π-conjugated spacers, since such spacers can mediate large electronic interactions between the donor and the acceptor, thereby enabling efficient energy- and electron-transfer reactions over long distances.[1–17] π-Conjugated spacers are quite promising for the construction of an extensive energy- or electron-transfer network in which the energy and electron movement can be guided in a predictable manner along these π-conjugated pathways. With this in mind, we developed zinc–free base hybrid diporphyrins in which two 10,20-diaryl-2,3,7,8,12,13,17,18-octaalkyl substituted porphyrins (see the structure of compound **8**) are bridged by 1,2-, 1,3-, and 1,4-bis(phenylethynyl)phenylene spacers,[16] since these bridges are useful in keeping donor and acceptor at well-defined geometries and in mediating large through-bond electronic interactions.

Recently, Lindsey *et al.* noted that the energy-transfer rate from the S_1-state of the zinc porphyrin to the free base porphyrin in diphenylethyne-linked diporphyrin is 17-fold larger in a 5,10,15,20-tetraphenylporphyrin (TPP)-type model[17] than a corresponding 5,15-diaryl octaalkyl porphyrin model[7] and proposed that this difference originates mainly from the reversal of the HOMO orbital of the porphyrin components which accompanies the change of porphyrin peripheral substituents. Their results seem to yield very useful information on the molecular design of an efficient energy-transfer network, since replacement of a 5,15-diaryl octaalkyl porphyrin by a TPP-type porphyrin may lead to much stronger through-bond electronic interactions, and thus the energy transfer along designed π-conjugated pathways would be enhanced. In this paper, we compare rates of the singlet–singlet energy transfer in bis(phenylethynyl)phenylene-bridged zinc–free base hybrid TPP-type diporphyrins **1–3(ZH)** (M^1 = Zn, M^2 = H_2) with those in the corresponding 10,20-diaryl-2,3,7,8, 12,13,17,18-octaalkyl substituted porphyrin models. Here, novel porphyrin dimers **1–3(ZH)** were prepared by a Pd-catalyzed coupling reaction of ethynyl-substituted porphyrin **7** with diiodobenzenes in moderate to high yields. We also found that a similar reaction with 1,2,4,5-tetraiodobenzene gave the corresponding porphyrin tetramer **10(Z4)**.

Results and discussion

Following Lindsey's method,[11] ethynyl-substituted porphyrin **7** was prepared quantitatively *via* trimethylsilyl-protected porphyrin **6**, which was, in turn, prepared by the cross condensation of 3,5-di-*tert*-butylbenzaldehyde, dipyrrylmethane (**4**),[18] and 4-[2-(trimethylsilyl)ethynyl]benzaldehyde (**5**)[19] followed by separation over a silica gel column in 15% overall yield. Coupling of **7** with 1,2-, 1,3-, and 1,4-diiodobenzenes with aid of $Pd_2(dba)_3$ and $As(Ph)_3$ catalysts[11] provided **1–3(ZZ)** (M^1 = M^2 = Zn) in 49%, 55%, and 84% yields, respectively (Scheme 1).

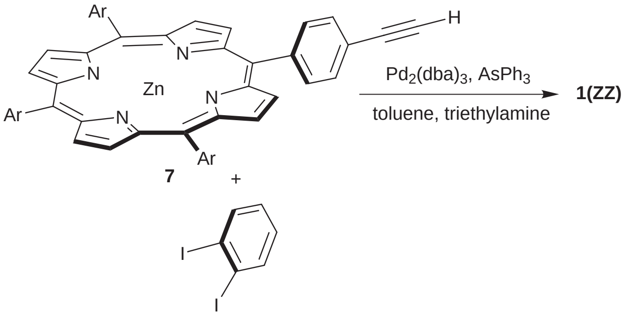

Scheme 1 Synthesis of **1(ZZ)**.

The reaction with 1,4-diiodobenzene was found to be almost completed within 24 h but the reaction with 1,2-diiodobenzene needed more than a week. These coupling reactions proceeded nicely without the formation of noticeable amounts of byproducts and product separation was relatively easy. After these bis-zinc porphyrins were demetalled to **1–3(HH)** by concentrated HCl, zinc–free base hybrid diporphyrins **1–3(ZH)**

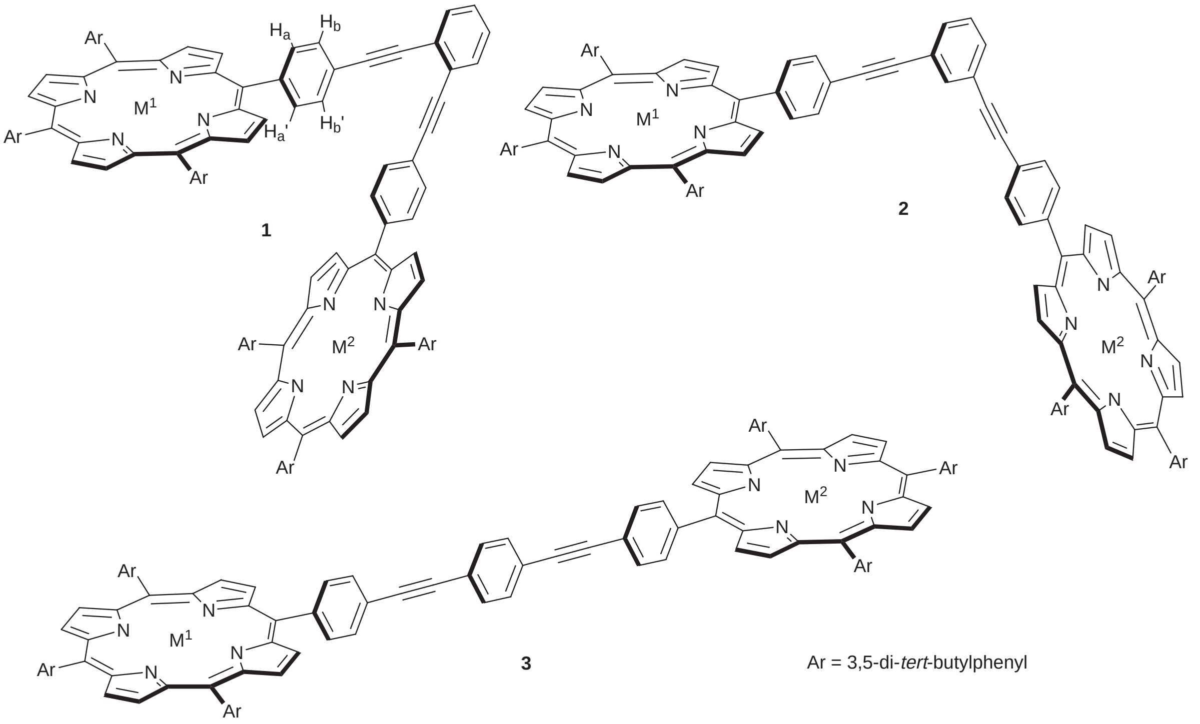

1

2

3

Ar = 3,5-di-*tert*-butylphenyl

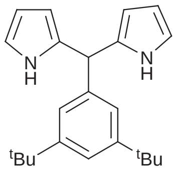

4

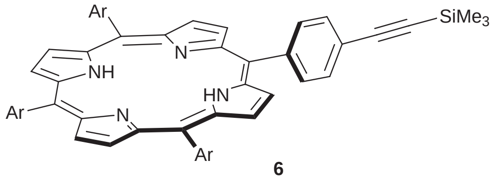

6

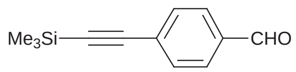

5

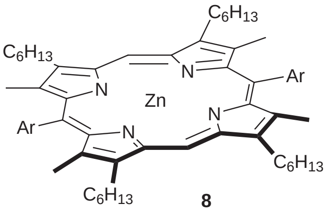

8

were prepared by partial zinc-insertion into **1**–**3(HH)** followed by separation over a silica gel column in 30–40% yields. All these porphyrins are characterized by 500 MHz ^{1}H NMR and FAB mass spectra. In the ^{1}H NMR spectrum of **1(ZZ)**, H_a, H_a', H_b, and H_b' protons appear as two slightly broad doublets at 8.26 and 8.10 ppm ($J = 8.0$ Hz), indicating that the rotation of an ethynylphenyl-substituted zinc porphyrin was faster than the NMR timescale at room temperature.

To expand this coupling strategy, the reaction of **7** with 1,2,4,5-tetraiodobenzene was also attempted. After the reaction under similar conditions was allowed to continue for a week at room temperature, the reaction mixture was separated by silica gel column and size-exclusion HPLC, giving dimeric product **9** (28%) and porphyrin tetramer **10** (16%) (Scheme 2). Consistent with the symmetric structure, the 500 MHz ^{1}H NMR spectrum of **10** displays a single set of protons for the ethynylphenyl-substituted zinc porphyrin and a singlet peak at 8.27 ppm for H^a at the central aromatic bridge. After demetallation to the free base form, its molecular weight was confirmed by MALDI-TOF mass method that revealed a peak at 3973.7 (Calcd. for $C_{286}H_{310}N_{16}$, 3971.3) (Fig. 1).[20] The cyclic geometry of the tetramer **10** seems interesting in view of its similarity to the supramolecular arrangement of photosynthetic antennae and detailed studies on rapid energy transfer within tetrameric or larger multi-porphyrin arrays are in progress in our laboratories and will be reported elsewhere. A similar coupling reaction of **7** with hexaiodobenzene was attempted but failed probably due to the very low solubility of the substrate.

The absorption spectra of **1**–**3(ZH)** were essentially the superposition of those of zinc porphyrin and free base porphyrin components, indicating negligible electronic interactions in the ground state. In the steady-state fluorescence spectra (Fig. 2), however, the fluorescence intensity of the zinc porphyrin is strongly reduced whereas that of the free base porphyrin is enhanced, showing the singlet excitation energy transfer from the zinc porphyrin to the free base porphyrin.[7–11,17,21–24] The fluorescence from the zinc porphyrin is quenched in the order **1(ZH)** > **2(ZH)** ~ **3(ZH)**, presumably reflecting the order of the intramolecular energy transfer from the zinc porphyrin to the free base porphyrin.

Fig. 3 shows the time-resolved fluorescence spectra[25] of **1(ZH)** taken by excitation at 532 nm in THF. The fluorescence emission at the early stage is assigned as being primarily due to the emission from the zinc porphyrin. Decay of the zinc porphyrin was followed by an increase in the free base porphyrin fluorescence. Time indicated in Fig. 3 shows the time difference from the best instrument response function time. Essentially the same time-resolved fluorescence spectra were observed for **2(ZH)** and **3(ZH)**. The fluorescence decay time constants of the zinc porphyrin in THF have been determined by a time-

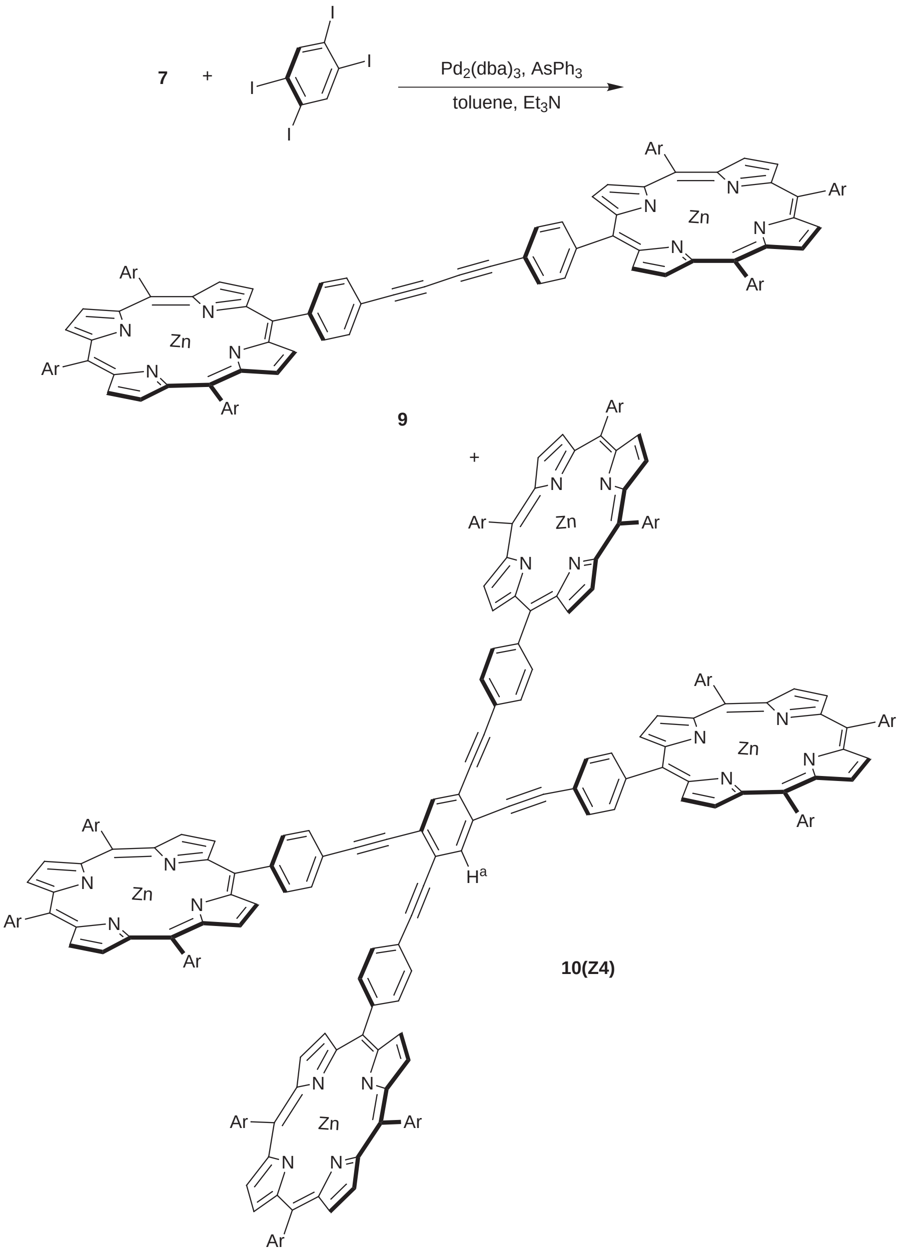

Scheme 2 Synthesis of porphyrin tetramer **10(Z4)**.

correlated single photon counting method. Fig. 4(A) displays the fluorescence decay of **1(ZH)** monitored at 600 nm. This fluorescence decay curve can be fitted satisfactorily with a biexponential function of 62 ps (99%) and 2.5 ns (1%) time constants, indicating practically a single exponential decay. The minor lifetime component may be interpreted in terms of adventitious impurities. Similarly the fluorescence decay times have been determined to be 197 ps and 145 ps for **2(ZH)** and **3(ZH)**, respectively (Table 1). In addition, the fluorescence increase time of the free base porphyrin has been measured by monitoring the emission at 710 nm where only the free base porphyrin emits fluorescence (Fig. 4(B) for **1(ZH)**). Determined fluorescence increase times are 49 ps, 194 ps, and 148 ps for **1**–**3(ZH)**, respectively, almost in agreement with the fluorescence decay time results. Since the fluorescence decay times are usually more reliable than the fluorescence increase times, we used the former values in calculating the rate of the energy transfer (k_{EN}) according to eqn. (1), where τ is the fluorescence decay

$$k_{EN} = \frac{1}{\tau} - \frac{1}{\tau_0} \qquad (1)$$

time of the zinc porphyrin in **1**–**3(ZH)** and τ_0 is the fluorescence decay time of the reference molecule (2.0 ns). Eqn. (1) gives 1.5×10^{10} s^{-1}, 4.6×10^{9} s^{-1}, and 6.4×10^{9} s^{-1} for k_{EN} in for **1**–**3(ZH)**. These rates are considerably larger than the rates of the corresponding 5,15-diaryl octaalkyl porphyrin counterparts; 4.4×10^{9} s^{-1}, 5.7×10^{8} s^{-1}, and 5.7×10^{8} s^{-1} for 1,2-, 1,3- and 1,4-bis(phenylethynyl)phenylene-bridged models, **11**, **12**, and **13**, respectively.[16] Thus it is now concluded that the change of a porphyrin subunit from a 10,20-diaryl octaalkyl porphyrin to a TPP-type porphyrin results in a rate enhancement of 3.4-, 8.1- and 11-fold for 1,2-, 1,3- and 1,4-isomers, respectively.

Two major mechanisms have been considered for singlet–singlet energy transfer. The Förster mechanism operates *via* Coulombic interaction between transition dipole moments of donor and acceptor.[26] In this mechanism, the rates of energy transfer are expressed in terms of the geometrical parameters (the centre-to-centre distance and the orientation factor) of the transition dipole moments, the spectral overlap integral between the normalized fluorescence spectrum of the donor and the absorption spectrum of the acceptor, and the fluorescence lifetime of the donor. In a comparison of the two diporphyrin sets, the centre-to-centre distances and the orientations are nearly the same, and the spectral overlap is

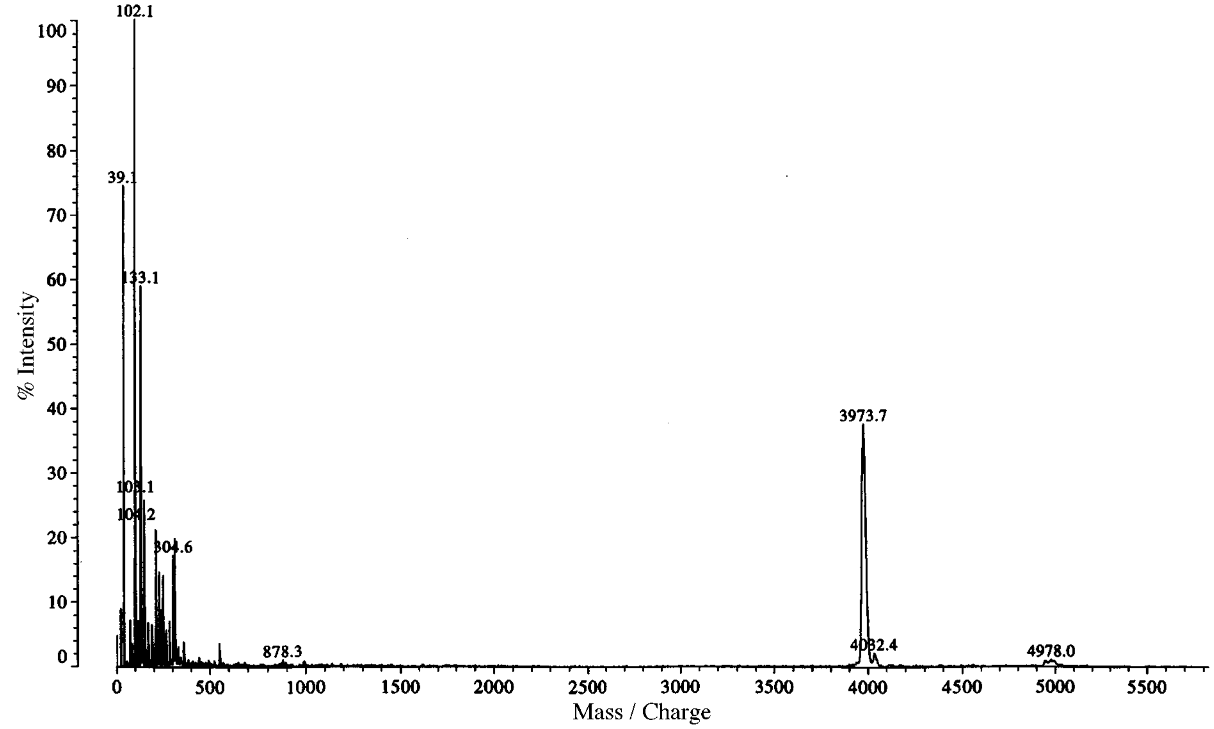

Fig. 1 MALDI-TOF Mass spectrum of **10(H4)**.

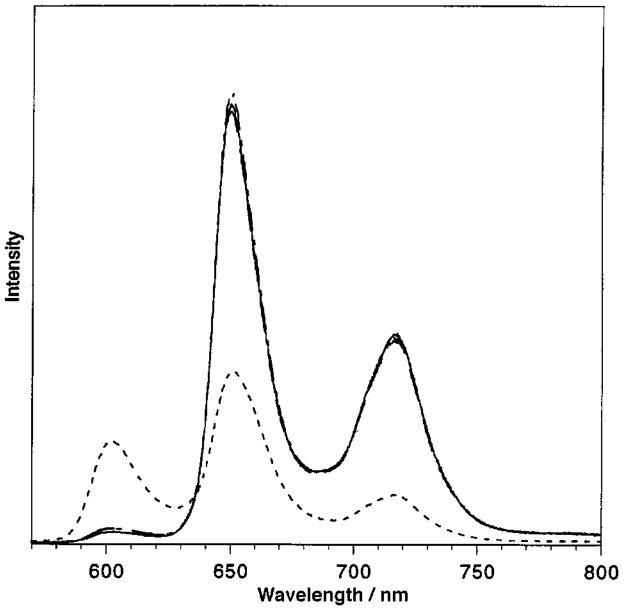

Fig. 2 Steady-state fluorescence spectra of **1–3(ZH)** in THF. **1(ZH)** (——), **2(ZH)** (–––), **3(ZH)** (— — —), and a 1 : 1 mixture of zinc porphyrin and free base porphyrin (····).

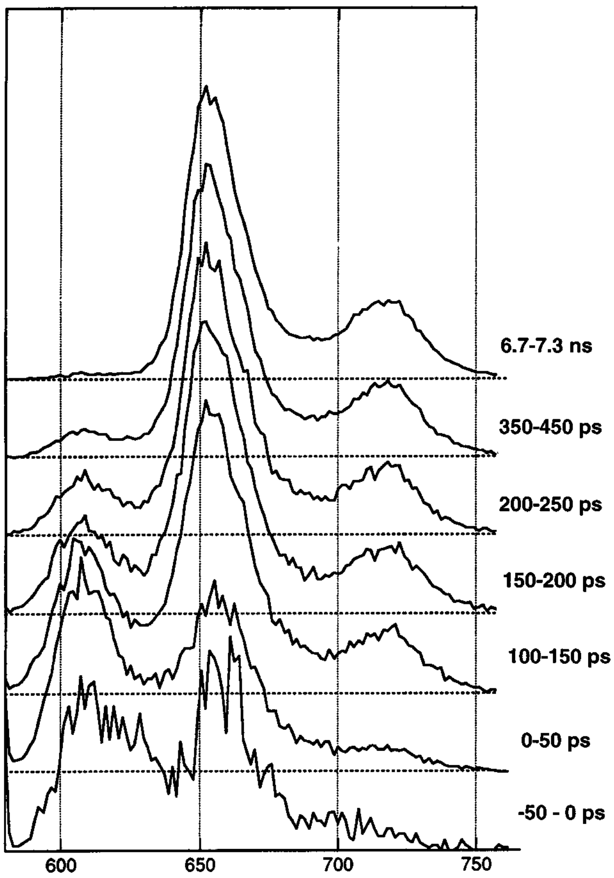

Fig. 3 Time-resolved fluorescence spectra of **1(ZH)** in THF ($\lambda_{ex} = 532$ nm).

also similar; 3.8×10^{-14} mmol^{-1} cm^6 for **1–3(ZH)** and 3.5–4.7 $\times 10^{-14}$ mmol^{-1} cm^6 for the 10,20-diaryl octaalkyl diporphyrin,[16] and the fluorescence lifetimes of the donor are also similar; 2.0 ns for the former and 1.46 ns for the latter. Therefore, the Förster mechanism alone cannot explain the observed energy transfer rate enhancement in **1–3(ZH)** compared with those in **11–13**. The other is the Dexter mechanism which requires an electronic exchange interaction between the donor and acceptor.[27] In this mechanism, the observed rate enhancement can be considered to be due to the increased electronic interaction of the donor and acceptor. In the 10,20-diaryl octaalkyl porphyrin, β-alkyl groups flanking the aryl bridge keep the bridge's geometry nearly perpendicular to a porphyrin plane, thereby minimizing the electronic interactions between the porphyrin and the bridge. Such a strict conformational restriction is weaker in **1–3(ZH)**, thus giving rise to increased electronic interactions between the porphyrins. Another factor, which can be more important for the enhanced through-bond electronic interaction, may be stemming from the HOMO

Table 1 Rates of energy transfer

Compound	τ/ps[a]	k_{EN}[b]/s^{-1}	Compound	τ/ps[c]	k_{EN}/s^{-1}	Enhancement[d]
1(ZH)	62	1.5×10^{10}	**11**	195	4.4×10^{9}	3.4
2(ZH)	197	4.6×10^{10}	**12**	793	5.7×10^{9}	8.1
3(ZH)	145	6.4×10^{10}	**13**	796	5.7×10^{9}	11

[a] The decay lifetime of the fluorescence of the zinc porphyrin at 600 nm. [b] Rate of singlet energy transfer calculated on the basis of the fluorescence lifetime according to eqn. (1). [c] The decay lifetime of the fluorescence of the zinc porphyrin at 585 nm. [d] The ratio of the rate of the singlet energy transfer in the TPP-type compounds **1**–**3(ZH)** to those in **11**–**13**.

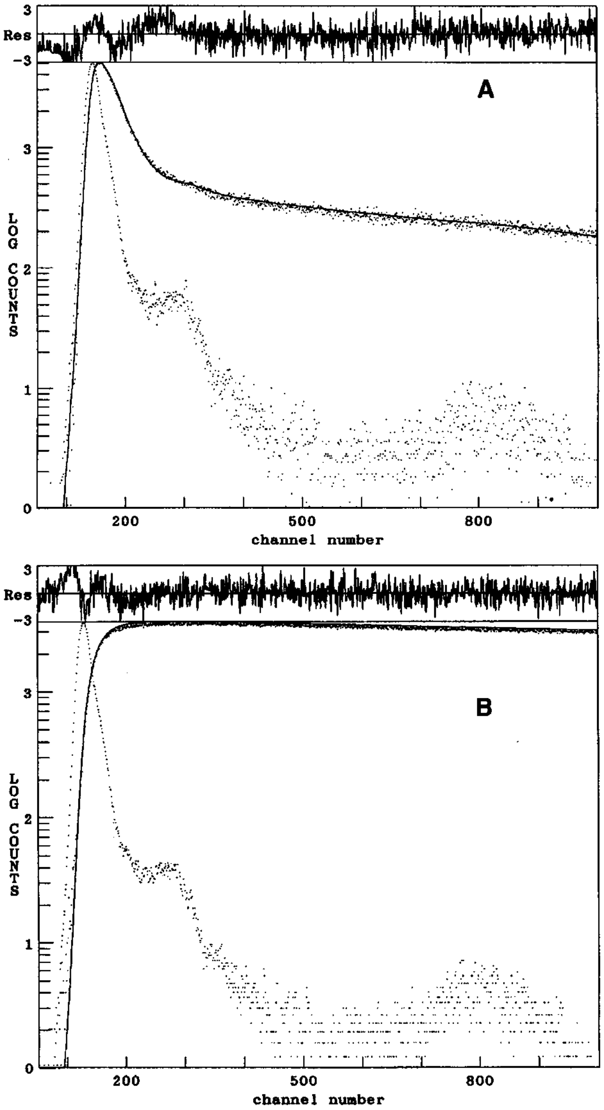

Fig. 4 Fluorescence decay curve of **1(ZH)** in THF monitored at 600 nm (A) and at 710 nm (B) (λ_{ex} = 532 nm). The top graphs give the residuals to the biexponential fits that are indicated by solid lines.

orbital reversal from a_{1u} in a 10,20-diaryl octaalkylporphyrin to a_{2u} in a TPP-type porphyrin.[17] The a_{2u} orbital has substantial electron density on the *meso*-carbon atoms, where the bridge is appended. The same explanation has been presented for the difference in the singlet energy transfer rates between the TPP model and the 2,3,7,8,12,13,17,18-octaethylporphyrin (OEP) model of the diphenylethynyl-bridged zinc–free base hydride diporphyrins.

Relatively small rate enhancement in **2(ZH)** compared to that in **3(ZH)** may reflect its nonconjugated electronic character. In other words, the extent of the through-bond electronic interaction in the overall electronic interaction is smaller in **2(ZH)**, which leads to the smaller rate enhancement. In **1(ZH)**, the two porphyrins are held at a rather proximate geometry and thus substantial electronic interactions are provided also by the through-space interaction (the Förster mechanism). This is also the case for the corresponding 10,20-diaryl octaalkyl porphyrin model, for which we estimated the through-space interaction to be one order of magnitude larger than the through-bond interactions.[16] In this situation, the increase of the through-bond electronic interaction upon the change of the OEP-type to the TPP-type porphyrin results in smaller rate enhancement.

In summary, larger through-bond electronic interactions between the TPP-type porphyrins over bis(1,4-phenylethynyl)-phenylene spacers in comparison with the OEP-type porphyrins are manifest in the efficient singlet energy transfer. The rate enhancement depends on the geometry of the two porphyrins, reflecting the magnitude of the through-bond electronic interaction, and is larger in a model where the through-bond interactions are larger in the overall electronic interaction. Thus, the rate enhancement is expected to depend on the geometry of the diporphyrins and to be in the order of **3(ZH)** > **2(ZH)** > **1(ZH)** as is actually observed. Extension of these electronically communicating subunits to the electron-transfer system is now ongoing. A Pd-catalyzed coupling strategy is very useful in constructing porphyrin networks, even for a porphyrin tetramer, in a one-pot procedure.

Experimental

All solvents and reagents were purified by standard methods before use. The instruments were previously reported.[16] The ^{1}H NMR spectra were recorded on a 500 MHz JEOL α-500 spectrometer. The mass spectra were recorded on a JEOL HX-110 spectrometer using positive FAB ionization method (accelerating voltage 1 kV, Xe atom as the primary ion source, and a mixture of *m*-nitrobenzyl alcohol and $CHCl_3$ as the FAB matrix). MALDI-TOF mass was measured on a KRATOS PC-KOMPACT SHIMADZU MALDI-4. The MALDI-TOF mass method has been recently reported to be particularly effective in detecting the parent peak of large porphyrin arrays.[20] MALDI-TOF MS experiments were carried out with a sinapinic acid matrix and an internal standard of bovine insulin (m/z = 5734).

5,15,20-Tris(3,5-di-*tert*-butylphenyl)-10-[4-(trimethylsilylethynyl)phenyl]porphyrin (6)

This compound was prepared by the condensation of 3,5-di-*tert*-butylbenzaldehyde and **5** with **4** followed by oxidation with *p*-chloranil in an overall yield of 15%. ^{1}H NMR ($CDCl_3$) δ 8.89 (s, 4H, β-pyrrole), 8.88 (d, 2H, β-pyrrole, J = 5.0 Hz), 8.80 (d, 2H, β-pyrrole, J = 5.0 Hz), 8.17 (d, 2H, ArH, J = 8.0 Hz), 8.07 (m, 8H, ArH), 7.86 (d, 2H, ArH, J = 8.0 Hz), 7.79 (m, 4H, ArH), 1.52 (m, 54H, *tert*-butyl-H), 0.38 (s, 9H, $SiMe_3$), and −2.71 (broad, 2H, inner-NH): FAB MS m/z 1049; Calcd. for $C_{73}H_{86}N_4Si$, 1048.

Zinc(II)-5,15,20-tris(3,5-di-*tert*-butylphenyl)-10-(4-ethynylphenyl)porphyrin (7)

This compound was prepared by desilylation of **6** with K_2CO_3 and subsequent zinc insertion. ^{1}H NMR ($CDCl_3$) δ 9.01 (s, 4H, β-pyrrole), 9.00 (d, 2H, β-pyrrole, J = 4.0 Hz), 8.92 (d, 2H, β-pyrrole, J = 4.0 Hz), 8.21 (d, 2H, ArH, J = 8.0 Hz), 8.09 (d, 2H, ArH, *J* = 8.0 Hz), 8.08 (d, 2H, ArH, *J* = 2.0 Hz), 7.88 (d, 2H, ArH, *J* = 2.0 Hz), 7.80 (t, 2H, ArH, *J* = 2.0 Hz), 7.79 (t, 1H, *J* = 2.0 Hz), 3.47 (s, 1H, acetylene-H), and 1.52 (m, 54H, *tert*-butyl-H): FAB MS *m*/*z* 1039; Calcd. for $C_{70}H_{76}N_4Zn$, 1039.

1,4-Bis{4-[zinc(II)-5,15,20-tris(3,5-di-*tert*-butylphenyl)-10-porphinyl]phenylethynyl}benzene (3(ZZ))

Ethynyl-substituted porphyrin **7** (51.8 mg, 50 µmol) and 1,4-diiodobenzene (9.0 mg, 27 µmol, 0.10 M stock solution in toluene) were dissolved in 20 mL of toluene–triethylamine (5 : 1). The reaction vessel headspace including the condenser was deaerated with a high flow rate of argon for 10 min. The solution was then deaerated by gently bubbling argon through the solution for 30 min. Then tris(dibenzylideneacetone)-dipalladium(0) ($Pd_2(dba)_3$, 3.3 mg) and triphenyl arsine ($AsPh_3$, 8.5 mg) were added. After 24 h the reaction mixture was concentrated to dryness and purified by flash column chromatography (silica, 2 cm diameter × 6 cm long, toluene–hexane = 1/2). The product was further purified by recrystallization from CH_2Cl_2 and methanol to give **3(ZZ)** (45.2 mg, 21 µmol, 84%): ^1H NMR ($CDCl_3$) 9.02 (m, 12H, β-pyrrole), 8.98 (d, 4H, β-pyrrole, *J* = 5.0 Hz), 8.27 (d, 4H, ArH, *J* = 8.0 Hz), 8.11 (d, 8H, ArH, *J* = 2.0 Hz), 8.10 (d, 4H, ArH, *J* = 2.0 Hz), 7.97 (d, 4H, ArH, *J* = 8.0 Hz), 7.81 (t, 4H, ArH, *J* = 2.0 Hz), 7.80 (t, 2H, ArH, *J* = 2.0 Hz), 7.76 (s, 4H, center-ArH), and 1.53 (s, 108H, *tert*-butyl-H): FAB MS *m*/*z* 2150; Calcd. for $C_{146}H_{154}N_8Zn_2$, 2152; UV (THF) 427.5 (Soret), 557.5, and 597 nm.

Monozinc complex 3(ZH)

To a solution of **3(HH)** prepared by acidic demetallation of **3(ZZ)** in CH_2Cl_2 was added a saturated methanol solution of $Zn(OAc)_2$. After being checked by TLC analysis, the solution was treated with water, dried over Na_2SO_4, and concentrated to dryness. Separation by flash column chromatography (silica gel, toluene–hexane = 1/4) followed by recrystallization from CH_2Cl_2 and methanol gave **3(ZH)** in *ca.* 30% yield: ^{1}NMR ($CDCl_3$) *δ* 9.03 (m, 6H, β-pyrrole), 8.99 (d, 2H, β-pyrrole, *J* = 5.0 Hz), 8.92 (m, 6H, β-pyrrole), 8.88 (d, 2H, β-pyrrole, *J* = 4.0 Hz), 8.28 (d, 2H, ArH, *J* = 8.0 Hz), 8.27 (d, 2H, ArH, *J* = 8.0 Hz), 8.12 (d, 4H, ArH, *J* = 1.5 Hz), 8.11 (d, 4H, ArH, *J* = 2.0 Hz), 8.10 (d, 2H, ArH, *J* = 2.0 Hz), 8.09 (d, 2H, ArH, *J* = 2.0 Hz), 7.97 (d, 4H, ArH, *J* = 8.0 Hz), 7.82 (m, 4H, ArH), 7.81 (m, 2H, ArH), 7.76 (s, 4H, center-ArH), and 1.54 (s, 108H, *tert*-butyl-H): FAB MS *m*/*z* 2087; Calcd. for $C_{146}H_{156}N_8Zn$, 2088; UV (THF) 426.5 (Soret), 516.5, 555.0, 596.5, and 648 nm.

Compounds **1(ZZ)**, **1(ZH)**, **2(ZZ)**, and **2(ZH)** were synthesized by essentially the same procedure as described for **3(ZZ)** and **3(ZH)** except for a longer reaction time (a week) for the synthesis of **1(ZZ)**. Here the selected physical properties of these model compounds are reported.

1(ZZ): Yield 46%; ^1H NMR ($CDCl_3$) 8.94 (m, 16H, β-pyrrole), 8.26 (d, 4H, ArH, *J* = 8.0 Hz), 8.10 (d, 4H, ArH, *J* = 8.0 Hz), 8.04 (d, 4H, ArH, *J* = 2.0 Hz), 7.99 (d, 8H, ArH, *J* = 1.5 Hz), 7.82 (dd, 2H, center-ArH, *J* = 3.0 Hz and *J* = 3.5 Hz), 7.76 (t, 2H, ArH, *J* = 1.5 Hz), 7.69 (t, 4H, ArH, *J* = 1.5 Hz), 7.48 (dd, 2H, center-ArH, *J* = 3.5 Hz and 4.0 Hz), and 1.53 (s, 108H, *tert*-butyl-H); FAB MS *m*/*z* 2149, Calcd. for $C_{146}H_{154}N_8Zn_2$, 2152; UV (THF) 424.5 (Soret), 557, and 597 nm.

1(ZH): ^1H NMR ($CDCl_3$) 8.94 (m, 8H, β-pyrrole), 8.83 (m, 8H, β-pyrrole), 8.27 (d, 2H, ArH, *J* = 8.0 Hz), 8.26 (d, 2H, ArH, *J* = 8.0 Hz), 8.10 (d, 4H, ArH, *J* = 8.0 Hz), 8.04 (d, 2H, ArH, *J* = 2.0 Hz), 8.02 (d, 2H, ArH, *J* = 1.5 Hz), 7.99 (d, 4H, ArH, *J* = 2.0 Hz), 7.98 (d, 4H, ArH, *J* = 2.0 Hz), 7.82 (dd, 2H, center-ArH, *J* = 3.0 Hz and *J* = 3.5 Hz), 7.75 (t, 2H, ArH, *J* = 1.5 Hz), 7.69 (t, 4H, ArH, *J* = 2.0 Hz), 7.47 (dd, 2H, center-ArH, *J* = 3.5 Hz and *J* = 4.0 Hz), and 1.53 (s, 108H, *tert*-butyl-H): FAB MA *m*/*z* 2087; Calcd. for $C_{146}H_{156}N_8Zn$, 2088; UV (THF) 421.0 (Soret), 516.5, 555.0, 596.5, and 648 nm.

2(ZZ): Yield 55%; ^1H NMR ($CDCl_3$) 9.04 (m, 12H, β-pyrrole), 9.01 (d, 4H, β-pyrrole), 8.29 (d, 4H, ArH, *J* = 8.5 Hz), 8.13 (d, 8H, ArH, *J* = 2.0 Hz), 8.11 (d, 4H, ArH, *J* = 2.0 Hz), 8.05 (m, 1H, center-ArH), 8.00 (d, 4H, ArH, *J* = 8.0 Hz), 7.82 (t, 4H, ArH, *J* = 2.0 Hz), 7.81 (t, 2H, ArH, *J* = 1.5 Hz), 7.73 (dd, 2H, center-ArH, *J* = 1.5 Hz and *J* = 3.0 Hz), 7.53 (t, 1H, center-ArH, *J* = 8.0 Hz), and 1.55 (s, 108H, *tert*-butyl-H): FAB MS *m*/*z* 2150; Calcd. for $C_{146}H_{154}N_8Zn_2$, 2152; UV (THF) 426.5 (Soret), 557.5, and 597 nm.

2(ZH): ^{1}NMR ($CDCl_3$) 9.03 (m, 6H, β-pyrrole), 8.99 (d, 2H, β-pyrrole, *J* = 4.5 Hz), 8.92 (m, 6H, β-pyrrole), 8.89 (d, 2H, β-pyrrole, *J* = 4.5 Hz), 8.28 (d, 4H, ArH, *J* = 7.5 Hz), 8.12 (d, 4H, ArH, *J* = 2.0 Hz), 8.11 (d, 4H, ArH, *J* = 2.0 Hz), 8.10 (d, 2H, ArH, *J* = 1.5 Hz), 8.09 (d, 2H, ArH, *J* = 2.0 Hz), 8.00 (m, 1H, center-ArH), 7.98 (d, 4H, ArH, *J* = 7.5 Hz), 7.81 (t, 4H, ArH, *J* = 2.0 Hz), 7.80 (t, 2H, ArH, *J* = 1.5 Hz), 7.72 (dd, 2H, center-ArH, *J* = 1.5 Hz and *J* = 3.0 Hz), 7.52 (t, 1H, center-ArH, *J* = 7.5 Hz), and 1.54 (s, 108H, *tert*-butyl-H): FAB MS *m*/*z* 2088; Calcd. for $C_{146}H_{156}N_8Zn$, 2088; UV (THF) 425.5 (Soret), 516.0, 555.5, 596.0, and 648.5 nm.

Synthesis of porphyrin tetramer

A deaerated solution of **7** (19.9 mg, 19 µmol) and 1,2,4,5-tetraiodobenzene (2 mg, 3.4 µmol) in a mixture of dry toluene–triethylamine (6 mL, 5/1) was treated with $Pd_2(dba)_3$ (1.8 mg) and Ph_3As (6.8 mg) and the resulting solution was stirred at room temperature under argon in the dark. After being stirred for a week, the solution was concentrated to dryness and purified by flash column chromatography (silica, hexane–toluene = 3/1→1/1) to yield **9** and **10(Z4)**. The tetramer was finally purified by size-exclusion chromatography (Japan Analytical Industry Co. Ltd., recycling preparative HPLC instrument with a combination of JAIGEL-1H, JAIGEL-2H, and JAIGEL-2.5H columns in series). Yield of **10** (2.3 mg, 16% based on the amount of 1,2,4,5-tetraiodobenzene used).

9: ^{1}NMR ($CDCl_3$) *δ* 9.047 (d, β-pyrrole, 8H, *J* = 4.5 Hz), 9.028 (s, β-pyrrole, 8H), 8.980 (d, β-pyrrole, 8H, *J* = 4.5 Hz), 8.117 (d, 4H, ArH, *J* = 2 Hz), 8.100 (d, 4H, ArH, *J* = 2 Hz), 7.814 (t, 2H, ArH, *J* = 2 Hz), 7.802 (t, 4H, ArH, *J* = 2 Hz), and 1.54 (s, 108H, *tert*-butyl-H): FAB MS *m*/*z* 2074; Calcd. for $C_{140}H_{150}N_8Zn_2$, 2075.

10(Z4): ^{1}NMR ($CDCl_3$) *δ* 8.89–8.85 (m, 32H, β-pyrrole), 8.883 (broad d, 8H, ArH, *J* = 8 Hz), 8.273 (s, 2H, central Ar-H), 8.189 (broad d, ArH, 8H, *J* = 8 Hz), 8.037 (d, 8H, ArH, *J* = 2 Hz), 8.007 (d, 16H, ArH, *J* = 1.5 Hz), 7.764 (t, 4H, ArH, *J* = 2 Hz), 7.710 (t, 8H, ArH, *J* = 1.5 Hz), and 1.54 (s, 216H, *tert*-butyl-H); UV (THF) 426.5 (Soret, relative *ε*, 1.00), 558.0 (0.049), 598.2 (0.024) nm; Fluorescence (THF) 604.8 (relative intensity, 1.0) and 655.6 (0.71) nm.

The tetramer **10(Z4)** was treated with 6 M HCl to be demetallated to give free base tetramer **10(H4)** for the molecular weight determination by MALDI-TOF MS. **10(H4)**: ^{1}NMR ($CDCl_3$) 8.97 (m, 32H, β-pyrrole), 8.32 (d, 8H, ArH, *J* = 8 Hz), 8.27 (s, 2H, center-ArH), 8.19 (d, 8H, *J* = 8 Hz), 8.04 (d, 8H, *J* = 2.0 Hz), 8.01 (d, 16H, ArH, *J* = 1.5 Hz), 7.76 (t, 4H, ArH, *J* = 1.5 Hz), 7.71 (t, 8H, ArH, *J* = 2.0 Hz), 1.50 (m, 216H), and −2.73 (broad s, 8H, inner NH): MALDI-TOF MS *m*/*z* 3973.7; Calcd. for $C_{286}H_{310}N_{16}Zn_4$, 3971.3; UV (THF) 420.8 (Soret, relative *ε*, 1.00), 516.6 (0.049), 551.6 (0.031), 594.2 (0.015), and 648.6 (0.014) nm; Fluorescence (THF) 650.4 (relative intensity, 1.0) and 716.8 (0.46) nm.

Acknowledgements

We are grateful to Professor J. S. Lindsey of North Carolina State University for his helpful suggestions for the Pd-catalyzed coupling of ethyne-substituted porphyrin and iodobenzene derivatives. We also thank A. Nakano for the measurement of MALDI-TOF MS. This work was partly supported by Grant-in-Aids for Scientific Research from the Ministry of Education, Science, Sports, and Culture of Japan.

References

1 S. Kugimiya, T. Larzak and J.-M. Lehn, *J. Chem. Soc.*, *Chem. Commun.*, 1991, 1179.

2 A. C. Benniston, V. Goulle, A. Harriman, J.-M. Lehn and B. Marczinke, *J. Phys. Chem.*, 1994, **98**, 7798, and references cited therein.

3 A. Harriman and R. Ziessel, *Chem. Commun.*, 1996, 1707.

4 N. Holl, H. Port, H. C. Wolf, H. Strobel and F. Effenberger, *Chem. Phys.*, 1993, **176**, 215.

5 F. Würthner, M. S. Vollmer, F. Effenberger, P. Emele, D. U. Meyer, H. Port and H. C. Wolf, *J. Am. Chem. Soc.*, 1995, **117**, 8090.

6 H. Imahori, H. Higuchi, Y. Matsuda, A. Itagaki, Y. Sakai, J. Ojima and Y. Sakata, *Bull. Chem. Soc. Jpn.*, 1994, **67**, 2500.

7 A. Osuka, N. Tanabe, S. Kawabata, I. Yamazaki and Y. Nishimura, *J. Org. Chem.*, 1995, **60**, 7177.

8 S. Prathapan, T. E. Johnson and J. S. Lindsey, *J. Am. Chem. Soc.*, 1993, **115**, 7519.

9 R. W. Wagner and J. S. Lindsey, *J. Am. Chem. Soc.*, 1994, **116**, 9759.

10 J. Seth, V. Palaniappan, T. E. Johnson, S. Prathapan, J. S. Lindsey and D. F. Bocian, *J. Am. Chem. Soc.*, 1994, **116**, 10578.

11 R. W. Wagner, T. E. Johnson and J. S. Lindsey, *J. Am. Chem. Soc.*, 1996, **118**, 11166.

12 V. S.-Y. Lin, S. G. DiMangno and M. J. Therien, *Science*, 1994, **264**, 1105.

13 D. P. Arnold and L. J. Nitschinsk, *Tetrahedron*, 1992, **48**, 8781.

14 D. P. Arnold and G. A. Heath, *J. Am. Chem. Soc.*, 1993, **115**, 12197.

15 J. J. Gosper and M. Ali, *J. Chem. Soc.*, *Chem. Commun.*, 1994, 1707.

16 S. Kawabata, I. Yamazaki, Y. Nishimura and A. Osuka, *J. Chem. Soc.*, *Perkin Trans. 2*, 1997, 479.

17 J.-P. Strachan, S. Gentemann, J. Seth, W. A. Kalsbeck, J. S. Lindsey, D. Holten and D. F. Bocian, *J. Am. Chem. Soc.*, 1997, **119**, 11191.

18 C. H. Lee and J. S. Lindsey, *Tetrahedron*, 1994, **39**, 11427.

19 W. B. Austin, N. Bilow, W. J. Kelleghan and K. S. Y. Lau, *J. Org. Chem.*, 1981, **46**, 2280.

20 D. Fenyo, B. T. Chait, T. E. Johnson and J. S. Lindsey, *J. Porphyrins Phthalocyanines*, 1997, **1**, 93.

21 J. A. Anton, P. A. Loach and Govindjee, *Photochem. Photobiol.*, 1978, **28**, 235.

22 R. L. Brookfield, H. Ellul, A. Harriman and G. Porter, *J. Chem. Soc.*, *Faraday Trans. 2*, 1986, **82**, 219.

23 A. Osuka, K. Maruyama, I. Yamazaki and N. Tamai, *Chem, Phys. Lett.*, 1990, **165**, 392.

24 D. Gust, T. A. Moore, A. L. Moore, F. Gao, D. Luttrull, J. M. DeGraziano, X. C. Ma, L. R. Makings, S.-J. Lee, T. T. Trier, E. Bittersmann, G. R. Seely, S. Woodward, R. V. Bensasson, M. Rougèe, F. C. De Schryver and M. Van der Auweraer, *J. Am. Chem. Soc.*, 1991, **113**, 3638.

25 I. Yamazaki, N. Tamai, H. Kume, H. Tsuchiya and K. Oba, *Rev. Sci. Instrum.*, 1985, **56**, 1187.

26 T. Förster, *Discuss. Faraday Soc.*, 1959, **27**, 7.

27 D. L. Dexter, *J. Chem. Phys.*, 1953, **21**, 836.

Paper 8/08396G